Local optical spectroscopy of self-assembled quantum dots using a near-field optical fiber probe to induce a localized strain field

H. D. Robinson, M. G. Müller,[a] and B. B. Goldberg
Department of Physics, Boston University, Boston, Massachusetts 02215

J. L. Merz
Department of Electrical Engineering, Notre Dame University, South Bend, Indiana 46556

(Received 27 January 1998; accepted for publication 2 March 1998)

We introduce and demonstrate a novel operating mode in near-field optical microscopy. The tip is used to simultaneously optically probe the sample and induce a highly localized strain in the area under study by pushing the tip into the sample. From knowledge of total tip-sample compression and tip geometry, we estimate the magnitude of stress, and show that localized uniaxial-like stresses in excess of 10 kbar can be achieved. We apply this method to a sample of InAlAs self-assembled quantum dots. A blueshift of quantum dot emission lines consistent with estimates of the strain is observed, as well as a quenching of the photoluminescence with strain. © *1998 American Institute of Physics.* [S0003-6951(98)04017-0]

In this letter, we demonstrate a new mode of operation for the near-field scanning optical microscope[1,2] (NSOM) in which the NSOM tip, in addition to confining the collection of excitation light to a subwavelength region, is used to induce a localized strain directly below the tip, accomplished by pushing the tip into the surface. See schematic in Fig. 1. Experimental verification of the technique is done with self-assembled quantum dots (SADs)[3] for several reasons: (1) the dots are sufficiently small ($\sim 10-20$ nm) to be considered to be under uniform external strain; (2) the photoluminescence (PL) emission line from a single dot is very narrow ($<100\ \mu$eV)[4] assuring that small spectral shifts are easily detectable; and (3) the dots are very bright, facilitating the use of NSOM, which is intrinsically a low light signal technique.

The sample used in this experiment[5–8] consists of $In_{0.55}Al_{0.45}As$ SADs made by molecular beam epitaxy (MBE) in the Stranski–Krastanov growth mode[9,10] on $Al_{0.35}Ga_{0.65}As$, capped with a 10 nm GaAs layer atop an AlGaAs layer embedding the dots. The dot density is 2×10^{10} cm^{-2}, the average lateral dot size is 18 nm, and the sample has a peak emission around 1.88 eV. All data in this letter are taken at $T=4$ K.

Finding the precise form of the induced stress field associated with a specific tip-sample compression and its exact effect on optical properties is a very complicated problem, requiring intensive numerical calculations. This is beyond the scope of this letter, and here we merely present order-of-magnitude estimates of the relevant quantities for comparison to the data. We estimate the compression of the NSOM tip by considering it to be an assembly of slowly tapering homogeneous cylinders. For such a cylinder, the stress-strain relationship is to first order:

$$C=\frac{4L}{Y\pi ab}F, \tag{1}$$

where L is the cylinder length, a and b are the diameters at either end, Y is Young's modulus, C the compression, and F the axial force. For the tips used in this experiment, which were made short and wide with relatively uniform tapers we find, using $Y_{SiO_2}=72$ GPa[11] that $C/F\approx0.2$ nm/μN. This corresponds to $C/\sigma\approx1.0$ (nm of compression)/(kbar of stress). For longer, more typical tips[12] we find $C/F\approx0.3-0.8$ nm/μN, and $C/\sigma\approx0.25-0.80$ nm/kbar. We can assume that the sample compresses less than the tip, making the total compression in the range 1–2 nm/kbar.

Two mechanisms impose an upper limit to the stresses: (1) the finite compressive strength of glass and (2) buckling of the tip. The compressive strength of SiO_2 is at least 11 kbar.[11] Since only a very small volume of the tip has to endure the maximum stress involved, the actual limit is likely significantly higher. A simple model[13] for the buckling of a beam holds that the maximum axial force before any possibility of buckling is given by

$$F_{\max}=YAIk^2, \tag{2}$$

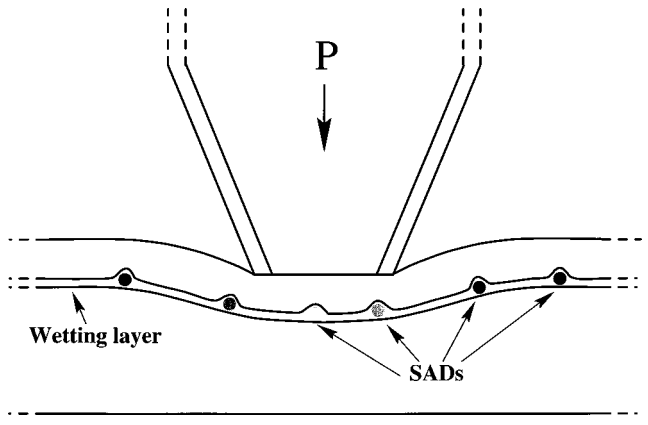

FIG. 1. The basic principle of the experiment. The tip induces a localized strain directly below itself, while simultaneously allowing spectroscopic study limited to that region. Lateral scanning is suspended to avoid abrasive damage to the tip.

[a]Present address: Fakultät für Physik und Astronomie, Universität Heidelberg, 69120 Heidelberg, Germany.

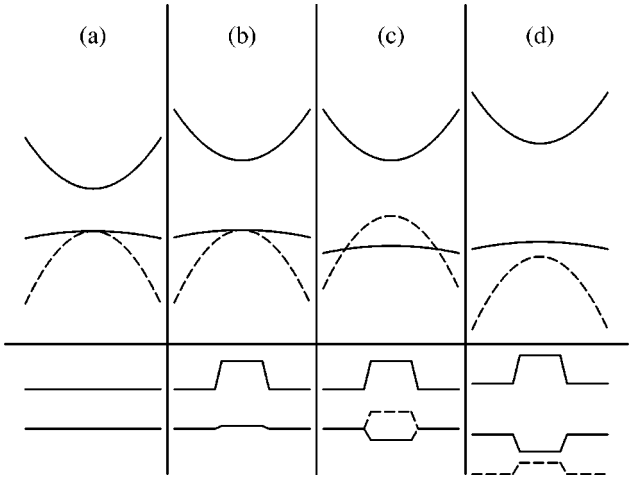

FIG. 2. Schematic of the behavior of band gap and band alignment under various types of stress. The upper part indicates the Γ-point band structure in the the stressed region and the lower part the spatial band alignment with surrounding material. (a) Unstressed bulk. (b) Hydrostatic compression. (c) Uniaxial compression. (d) Uniaxial compression, including the effect of carrier confinement and preexisting strain.

where A is the cross-sectional area of the beam, I the area moment of inertia of that cross section, and k the wave vector of the lowest lateral excitation of the beam consistent with the boundary conditions. For a typical tip, with length $L=750\ \mu$m and $r=5\ \mu$m, we get $F_{\max}=155\ \mu$N, which for our 250 nm aperture tip corresponds to 31 kbar, and naturally more for a smaller tip. The maximum stress achievable is then at least 10 kbar. Experimentally, it is possible to go to twice this value without damaging the tip.

The shift of band edges with strain are given in terms of the band-edge deformation potentials (a,b,d).[14] b and d govern the behavior under axial and shear strain, and vanish to first order for the conduction band. The hydrostatic deformation potentials, a_c and a_v, are difficult to measure independently, and in most cases only the total a is known.

In GaAs, where a_v and a_c are known independently,[15] hydrostatic strain mainly affects the conduction band, as $a_c \sim 10a_v$, the net effect being a blueshift of the excitons under compressive strain. Axial and shear strain split the heavy- and light-hole bands—as shown schematically in Fig. 2. For compressive uniaxial strain, the dominant mechanism here, the heavy-hole band is shifted down, and the light-hole band up. Due to carrier confinement and intrinsic strain in the dots and the wetting layer, such a splitting, although of opposite sign, is already present, and the external induced strain decreases it.

Using data for the $In_xAl_{1-x}As$ system[16–18] we estimate the band-gap shift (dE_g/dP) in our sample to be 14.0 meV/kbar for hydrostatic stress, and 9.1 meV/kbar for uniaxial stress along [001]. We expect the tuning rate in this experiment to lie between these values, though closer to the lower bound, as the strain should be predominantly uniaxial.

Two distinct methods were used to collect the data. In *illumination mode* the tip optically excites the sample locally, and the PL is collected with traditional far-field optics. In *collection mode* the far-field objective delivers the exciting light to the region around the tip, and the tip is used to collect PL only from the area directly beneath it. The important difference between these modes is the influence of carrier diffusion, which degrades spatial resolution in illumination mode, but not in collection mode. In Fig. 3 a comparison of data taken in the two modes is shown. Each line in these spectra can be attributed to emission from an individual quantum dot. Since many more dots are observed in illumination mode, we would expect to see significantly smaller spectral shifts for a given compression, as the less strained area surrounding the tip is then being probed.

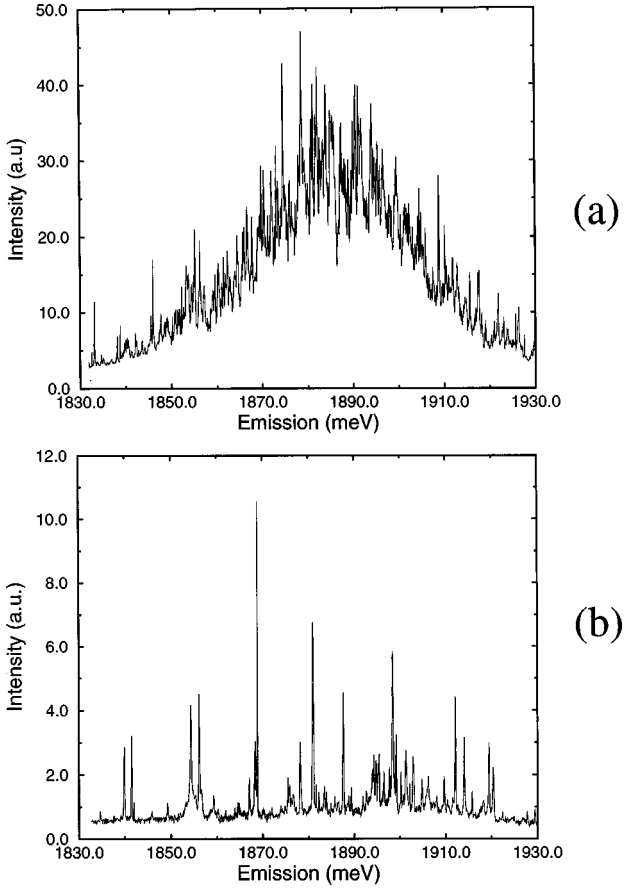

FIG. 3. Comparison between data taken in (a) illumination mode and (b) collection mode.

Figure 4 shows a typical data set taken in illumination mode. The compression is varied from 0 to 45 nm in steps of 10 and 5 nm. We note a linear blueshift of most emission lines at rates in the range 0.024–0.073 meV/nm, several

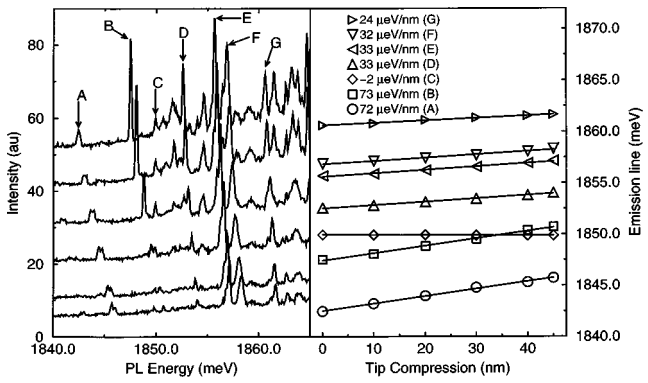

FIG. 4. Tuning of quantum dot PL lines with tip-sample compression. Data taken in illumination mode. Each line in the spectra at left represents ground state PL emission from a single quantum dot. Due to their varying position relative to the tip, each dot tunes at a different rate.

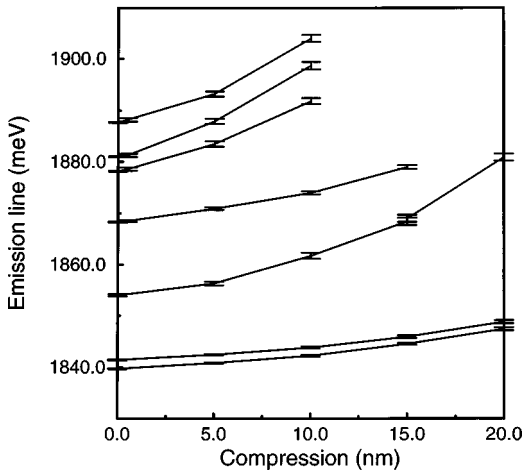

FIG. 5. Tuning of quantum dot PL lines with tip-sample compression. Data taken in collection mode.

times slower than the estimated rate for the dots experiencing the hardest strain, as expected. The tuning of selected lines from a similar data set taken in collection mode is shown in Fig. 5. The rates are in the range 0.2–2.4 meV/nm, which according to our estimates corresponds to 0.2–2.4 meV/kbar. This still falls short of the estimated lower bound. However, we have not taken into account several factors, such as the metal coating of the tip, the non-zero distance between tip and dots, and the fact that the barrier material is stiffer than the dot material, all of which would reduce the estimated tuning rates.

The strong nonlinearity in the Fig. 5 cannot be due to nonlinearities in the relationship between stress and band structure, which is linear to a good approximation below $\sim$40 kbar. We believe it is due to the presence of an angle between the flat end of the NSOM tip and the sample surface, resulting in an uneven strain as they come in contact with each other.[19]

Another effect we see in the data is quenching of the PL with increasing compression. This effect is particularly strong in collection mode, where no luminescence is observed for compressions larger than 25 nm. We ascribe the quenching to the potential gradient induced by the inhomogeneous strain. Since all data shows a blueshift of the PL line, this gradient will always cause excitons to move away from the tip, providing a simple explanation for the quenching in collection mode. It is harder to explain the presence of this effect in illumination mode. Since a affects mainly the conduction band, and b and d only the valence band, it is reasonable to assume that the character of the strain-induced potentials experienced by electrons and holes are very different. This, coupled with the fact that electrons have a larger mobility and therefore a faster escape rate could lead to a spatial separation of electrons and holes, reducing the exciton capture rate into and subsequent recombination from the dot states. Other effects that may be important are the direct-to-indirect gap transition, or the possibility that valence band mixing will make the ground state hole p-like, both of which would cause a quenching of the photoluminescence as observed.

The main difficulty with this mode of operation is determining the relation between tip-sample compression and actual stress. Once the form of the strain field has been calculated, however, calibration can be done using a better known system than the one in this experiment, such as a GaAs/AlGaAs quantum well. Since tips of the same size generally will have a similar shape, this calibration will be valid for other material systems if adjustments for the different elastic constants are made, and if the tip can be made sufficiently perpendicular to the sample. Efforts in this area are underway.

This localized strain technique adds a new degree of freedom to NSOM experiments. Not only can the magnitude of strain be varied, but the type of strain can also be changed, since this varies with the distance to the axis of the tip. The effect of strain gradients can also be studied by varying the the tip size. In light of its high experimental difficulty and low signal levels, NSOM often presents a relatively small advantage over far-field techniques such as confocal microscopy. The ability to regulate a local strain field in the area under optical study may help expand the number of applications where the use of NSOM can be justified.

This work was supported by NSF Grant No. DMR-9701958. The authors gratefully acknowledge P. M. Petroff, whose laboratory produced the sample used for these studies. They also thank Uma Venkateswaran and David Broido for helpful discussions.

[1] E. Betzig and J. K. Trautman, Science **257**, 189 (1992).
[2] R. Toledo-Crow, P. C. Yang, Y. Chen, and M. Vaez-Iravani, Appl. Phys. Lett. **60**, 2957 (1992).
[3] P. M. Petroff and S. P. Denbaars, Superlattices Microstruct. **15**, 15 (1994).
[4] J.-Y. Marzin, J.-M. Gérard, A. Israël, D. Barrier, and G. Bastard, Phys. Rev. Lett. **73**, 716 (1994).
[5] S. Fafard, R. Leon, J. L. Merz, and P. M. Petroff, Phys. Rev. B **52**, 5752 (1995).
[6] R. Leon, S. Fafard, D. Leonard, J. L. Merz, and P. M. Petroff, Science **267**, 1966 (1995).
[7] R. Leon, S. Fafard, D. Leonard, J. L. Merz, and P. M. Petroff, Appl. Phys. Lett. **67**, 521 (1995).
[8] P. D. Wang, J. L. Merz, S. Fafard, R. Leon, D. Leonard, G. Medeiros-Ribeiro, M. Oestrich, P. M. Petroff, K. Uchida, N. Miura, H. Akiyama, and H. Sakaki, Phys. Rev. B **53**, 16458 (1995).
[9] I. N. Stranski and L. V. Krastanow, Akad. Wiss. Lit. Mainz Abh. Math. Naturwiss. Kl. **146**, 797 (1939).
[10] L. Goldstein, F. Glas, J.-Y. Marzin, M. N. Charasse, and G. Le Roux, Appl. Phys. Lett. **47**, 1099 (1985).
[11] *Handbook of Chemistry & Physics*, 1st student ed. (CRC, Boca Raton, FL, 1988), p. F-32.
[12] G. A. Valaskovic, M. Holton, and G. H. Morrison, Appl. Opt. **34**, 1215 (1995).
[13] S. P. Timoshenko and J. M. Gere, *Theory of elastic stability*, 2nd ed. (McGraw–Hill, New York, 1961).
[14] G. E. Pikus and G. L. Bir, Sov. Phys. Solid State **1**, 136 (1959).
[15] D. D. Nolte, W. Walukiewicz, and E. E. Haller, Phys. Rev. Lett. **59**, 501 (1987).
[16] Landott-Börnstein, *Numerical Data and Functional Relationships in Science and Technology* (Springer, Berlin, 1982), Vols. III/17 and III/22.
[17] L. Pavesi, R. Houdré, and P. Giannozzi, J. Appl. Phys. **78**, 470 (1995).
[18] M. Krieger, H. Sigg, N. Herres, K. Bachem, and K. Köhler, Appl. Phys. Lett. **66**, 682 (1995).
[19] M. J. Gregor, P. G. Blome, J. Schöfer, and R. G. Ulbich, Appl. Phys. Lett. **68**, 307 (1996).